Haptic Teleoperation of Multiple Unmanned Aerial Vehicles over the Internet

Dongjun Lee, Antonio Franchi, Paolo Robuffo Giordano, Hyoung Il Son, and Heinrich H. Bülthoff

***Abstract*— We propose a novel haptic teleoperation control framework for multiple unmanned aerial vehicles (UAVs) over the Internet, consisting of the three control layers: 1) UAV control layer, where each UAV is abstracted by, and is controlled to follow the trajectory of, its own kinematic virtual point (VP); 2) VP control layer, which modulates each VP's motion according to the teleoperation commands and local artificial potentials (for inter-VP/VP-obstacle collision avoidance and inter-VP connectivity preservation); and 3) teleoperation layer, through which a remote human user can command all (or some) of the VPs' velocity while haptically perceiving the state of all (or some) of the UAVs over the Internet. Master-passivity/slave-stability and some asymptotic performance measures are proved. Semi-experiment results are presented to validate the theory.**

I. INTRODUCTION

Unmanned Aerial Vehicles (UAVs) are well-recognized for their promises to achieve many powerful applications with reduced cost/danger associated with the absence of human pilots onboard: e.g., pesticide-spraying, landscape survey, entertainment/games, ad-hoc communication network, and surveillance/reconnaissance, to name just a few. See [1].

Using multiple UAVs will further enhance these applications by merging the usual benefits of multirobot systems (e.g., higher performance in simultaneous spatial domain coverage, better affordability as compared to a single/bulky system, robustness against single point failure, etc.) with the motion flexibility of the aerial robots. This synergy can allow for many powerful multi-robot applications in the air such as cooperative/collaborative payload transport, remote manipulation, rescue, and remote sensing.

Given that many UAVs applications occur in unstructured/uncertain environments and fully-autonomous control design for such scenarios is typically infeasible/impossible, teleoperation of multiple UAVs would not only provide a superior performance via human's intelligent intervention, but also, perhaps, be the only viable option in many real multi-UAVs applications[1].

D. J. Lee is with the Department of Mechanical, Aerospace & Biomedical Engineering, University of Tennessee, Knoxville, TN 37996 USA. E-mail: djlee@utk.edu Phone: +1-865-974-5309, Fax: +1-865-974-5274.

A. Franchi, P. Robuffo Giordano, and H. I. Son are with the Max Planck Institute for Biological Cybernetics, Spemannstraße 38, 72076 Tübingen, Germany. E-mail: {antonio.franchi, paolo.robuffo-giordano, hyoungil.son}@tuebingen.mpg.de.

H. H. Bülthoff is with the Max Planck Institute for Biological Cybernetics, Spemannstraße 38, 72076 Tübingen, Germany, and with the Department of Brain and Cognitive Engineering, Korea University, Anam-dong, Seongbuk-gu, Seoul, 136-713 Korea. E-mail: hhb@tuebingen.mpg.de.

[1]Even for highly autonomous UAVs, some form of (multisensory) feedback of the remote UAVs' state and their environment would still be beneficial for the human user (e.g., better situational awareness, telepresence).

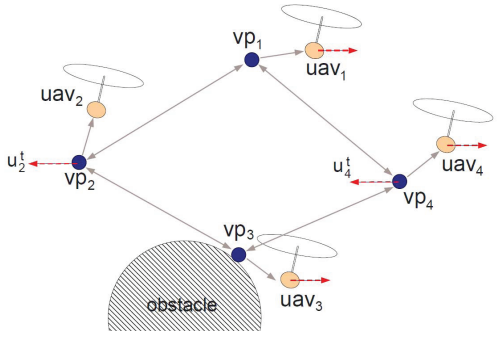

Fig. 1. Multi-UAVs teleoperation architecture with four real UAVs and their virtual points (VPs): gray solid arrows represent local information flows, while red dashed arrows that from/to the master site.

In this paper, we propose a novel haptic teleoperation control framework for multiple UAVs, which enables a single remote human user to stably teleoperate multiple distributed UAVs with some useful haptic feedback over the Internet with varying-delay, packet-loss, etc. Our framework consists of the following three control layers (see Fig. 1):

1) **UAV control layer**, that enforces each UAV to (unilaterally) track the trajectory of its own kinematic Cartesian virtual point (VP). For this, we assume availability of some reasonably-good trajectory tracking control laws for the UAVs (e.g. [2], [3], [4]), which then allow us to abstract the UAVs by their kinematic VPs, while bypassing the issues of the UAVs' low-level control (e.g., under-actuation);
2) **VP control layer**, that modulates the motion of the VPs in such a way that, as a whole, in a *distributed* manner, they behave as a deformable (multi-nodal) flying object, whose shape autonomously deforms according to local artificial potentials (designed for inter-VP/VP-obstacle collision avoidance and inter-VP connectivity preservation), while whose bulky motion is driven by the teleoperation velocity commands received from the master side;
3) **teleoperation layer**, that enables the human user to tele-drive some (or all) of the VPs, while haptically perceiving the state of some (or all) the real UAVs over the Internet. For this, passive set-position modulation (PSPM [5]) is adopted for its flexibility (e.g., allows for master-slave kinematic/dynamic dissimilarity and various forms of haptic feedback), guarantee of passivity over the Internet, and less conservative passifying action (thus, better performance).

Although there are many results for the single UAV control

(e.g. [2]-[4], [6]) and some results for the single UAV teleoperation (e.g. [7], [8]), those for the multiple UAVs teleoperation are rare. Among them, we think the followings are the most relevant ones: [9] proposes a multi-robot teleoperation scheme with precise slave formation control, which, yet, requires all-to-all communication among the slaves and addresses only the master-slave position-position teleoperation and fully-actuated robots, thus, not so suitable for underactuated/mobile UAVs with unbounded workspace [10]; [11] applies the results of [9] directly to the multiple UAVs (with collision avoidance), thus, inherits the same limitations of [9] as mentioned above; and [12] proposes a multiple wheeled mobile robots teleoperation scheme, that has some similarity with the current work (e.g., master-position/slave-velocity teleoperation via PSPM), yet, requires all-to-all slave communication (for precise slave formation control) and does not address collision-avoidance/connectivity-preservation among the slave robots.

The rest of this paper is organized as follows. Sec. II-A introduces some preliminary materials and details the three control layers: UAV control layer in Sec. II-B; VP control layer in Sec. II-C; and teleoperation layer in Sec. II-D. Sec. III presents semi-experiment results (i.e., real master and simulated UAVs). Sec. IV summarizes the paper with some comments on future research directions.

II. MULTIPLE UAVs TELEOPERATION CONTROL ARCHITECTURE

A. Preliminary

We consider N quadrotor-type unmanned aerial vehicles (UAVs), each with the following underactuated Lagrangian dynamics in $SE(3)$ [2][4]:

$$m_i\ddot{x}_i = -\lambda_i R_i e_3 + m_i g e_3 + \delta_i \quad (1)$$

$$J_i w_i + S(w_i)J_i w_i = \gamma_i + \zeta_i \quad (2)$$

with the attitude kinematic equation

$$\dot{R}_i = R_i S(w_i) \quad (3)$$

where $m_i > 0$ is the mass, $x_i \in \Re^3$ is the Cartesian position w.r.t. the NED (north-east-down) inertial frame with e_3 representing its down-direction, $\lambda_i \in \Re$ is the thrust along the body-frame e_3, $R_i \in SO(3)$ is the rotational matrix describing the body NED frame of UAV w.r.t. to the inertial NED frame, $w_i \in \Re^3$ is the angular rate of the UAV relatively to the inertial frame represented in the body frame, $J_i \in \Re^{3\times 3}$ is the UAV's inertia matrix w.r.t. the body frame, g is the gravitational constant, $\gamma_i \in \Re^3$ and $\zeta_i \in \Re^3$ are the attitude control and external torques w.r.t. the body frame, and $S(\star) : \Re^3 \to so(3)$ is the skew-symmetric operator defined s.t. for $a, b \in \Re^3$, $S(a)b = a \times b$.

We also consider a 3-degree-of-freedom (DOF) nonlinear Lagrangian haptic device as modeled by

$$M(q)\ddot{q} + C(q,\dot{q})\dot{q} = \tau + f \quad (4)$$

where $q \in \Re^3$ is the configuration, $M(q) \in \Re^{3\times 3}$ is the positive-definite/symmetric inertia matrix, $C(q,\dot{q}) \in \Re^{3\times 3}$ is the Coriolis matrix, and $\tau, f \in \Re^3$ are the control and human forces, respectively. Using skew-symmetricity of $\dot{M}-2C$, we can show that (4) is passive with the supply rate $[\tau + f]^T\dot{q}$.

Our goal is then to enable a remote human user to teleoperate N UAVs (1)-(3) via a single master haptic device (4) over the Internet. There are several interesting aspects/challenges to achieve this: 1) *large slave DOF:* humans can usually control well only a small DOF at the same time (e.g., 3-DOF for master (4)), yet, the slave system is of large DOF (i.e., $6N$-DOF for N UAVs); 2) *master-slave kinematic/dynamic dissimilarity [10]:* the master device (4) typically has a bounded workspace with full actuation (e.g., joystick), yet, the UAVs' workspace is unbounded (e.g., $E(3)$) and their dynamics is underactuated (e.g., only 1 control for 3-DOF (1)); and 3) *communication limitation:* substantial delay/loss is likely for the master-slave communication, particularly when established over the Internet, while the local communication among the UAVs, although possibly free from such significant delay/loss, is desired to be decentralized when the number of UAVs is large.

To address these challenges, as stated in Sec. I, we propose a novel control architecture for multiple UAV teleoperation consisting of the three control layers, UAV control layer, VP control layer, and PSPM-based teleoperation layer, each of which is detailed in the following three subsections.

B. UAV Control Layer

In this paper, we are mainly interested in teleoperating the 3-DOF Cartesian position of N UAVs, whose dynamics (1) is, yet, under-actuated (i.e., 1-DOF control λ_i for 3-DOF (1)), thus, defies most of the standard control techniques for achieving their teleoperation (e.g., for Sec. II-D) as well as other control objectives (e.g., for Sec. II-C). It would also be more desirable to "hide" this under-actuation issue from the human user so that s/he can focus more on the (high-level) teleoperation of the UAVs while not being distracted by this (low-level) under-actuation issue.

To circumvent this issue of under-actuation, we endow each UAV with a 3-DOF Cartesian VP (virtual point), $p_i \in \Re^3$. The human user will then teleoperate some (or all) of these N VPs over the Internet, while the real UAV's position, x_i, is tracking the trajectory of its own VP, p_i. See Fig. 1. Many trajectory tracking control laws are available for the UAVs (1)-(3) to achieve this (e.g., [2], [3] with input λ_i, γ_i; or [4] with λ_i, w_i). Note that, higher-order derivatives of p_i (e.g., $\dddot{p}_i$), usually necessary for those tracking control laws, can be numerically/cleanly computed here, since the VPs are simulated in software.

Abstracting the UAVs by their VPs and formulating our control objectives on these (simple) N VPs instead of the (complicated) UAVs, we can greatly simplify our control design for the VP-control layer (Sec. II-C) and for the teleoperation layer (Sec. II-D), while encapsulating the UAVs' under-actuation issue within the UAV control layer. This also implies that our multi-UAV teleoperation architecture, as proposed here, would be applicable to other types of mobile robots as well (e.g., humanoids), as long as they assume a

reasonably-good trajectory tracking control to follow their VPs. Thus, from now on, we assume that: 1) we have implemented a trajectory tracking control to make x_i to follow p_i; and 2) this control performs reasonably well, by keeping $||x_i - p_i||$ and $||\dot{x}_i - \dot{p}_i||$ small enough ($||x||^2 := x^T x$). How to control the motion of these N VPs is then the subject of the next Sec. II-C.

C. Distributed VP Control Layer

We consider N *first-order kinematic* VPs, with their Cartesian position $p_i \in \Re^3$ ($i = 1, 2, ..., N$). Our goal is to render these N VPs as a N-nodes deformable flying object in a *distributed manner*, so that their shape autonomously deforms reacting to the presence of obstacles, while their collective motion (and also possibly shape) is tele-controlled by the remote human user over the Internet, with the local communication among the VPs/UAVs distributed. See Fig. 1. As long as the UAV control layer in Sec. II-B ensures $||x_i - p_i||$ and $||\dot{x}_i - \dot{p}_i||$ to be small, these VPs' behaviors will be faithfully duplicated among the real UAVs.

To describe how the VPs are connected (and also communicating among themselves) to form the N-nodes flying object, we define the undirected connectivity graph G, with N VPs as its nodes and their connection (i, j) as its edges. Since G is undirected, $(i, j) \in \mathcal{E}(G)$ iff $(j, i) \in \mathcal{E}(G)$, where $\mathcal{E}(G)$ is the edge set of G. We assume G is connected and also dense[2] enough so that, with some suitably-defined inter-VP attractive/repulsive potentials on $\mathcal{E}(G)$, it can define the *un-deformed* shape of the N-nodes deformable object with no inter-VP separation or collision (e.g., rigid graph [13]). We also assume G to be time-invariant (e.g., no creation/elimination of edges over time). For some applications, a time-varying G may be useful (e.g., separation of N-nodes flying object to penetrate narrow passages and merge afterwards). See [14] for the case of such a time-varying G with constant master-slave delay and second-order dynamic VPs.

We implement the following kinematic evolution of VP on each UAV: for the i^{th} UAV,

$$\dot{p}_i(t) := u_i^t + u_i^c + u_i^o \tag{5}$$

where

1) $u_i^c \in \Re^3$ embeds the inter-VP collision avoidance and connectivity preservation, as defined by

$$u_i^c := -\sum_{j \in \mathcal{N}_i} \frac{\partial \varphi_{ij}^c(||p_i - p_j||^2)^T}{\partial p_i} \tag{6}$$

where φ_{ij}^c is a certain artificial potential function to create attractive action if $||p_i - p_j||$ is large, and repulsive action if $||p_i - p_j||$ small, and

$$\mathcal{N}_i := \{j \mid (j, i) \in \mathcal{E}(G)\}$$

i.e. connectivity neighbors of the i^{th} VP;

2) $u_i^o \in \Re^3$ is the obstacle avoidance action as given by

$$u_i^o := -\sum_{r \in \mathcal{O}_i} \frac{\partial \varphi_{ir}^o(||p_i - p_r^o||)^T}{\partial p_i} \tag{7}$$

where $\mathcal{O}_i$ is the set of obstacles of the i-th VP with p_r^o being the position of the r^{th} obstacle in $\mathcal{O}_i$, and φ_{ir}^o is a certain artificial potential, which produces repulsive action if $||p_i - p_r^o||$ is small, smoothly converges to zero as $||p_i - p_r^o|| \to d$, and stays zero with $||p_i - p_r^o|| \geq d$, to make the effect of obstacles for each VP gradually emerge/disappear when they move closer/farther from the VP than $d > 0$ (see Fig. 2);

3) $u_i^t \in \Re^3$ will contain the teleoperation command for the "control" subset $\mathcal{N}_t \subset \{1, 2, ..., N\}$ among the N VPs, to enable a remote human user to tele-drive the Cartesian velocity of those VPs in $\mathcal{N}_t$ and, consequently, that of the N-nodes flying object over the Internet (to be designed in Sec. II-D).

Here, both the inter-VP potential φ_{ij}^c and the VP-obstacle potential φ_{ij}^o are designed s.t.: 1) they are distance-based (i.e. $\varphi_{ij}^c(||p_i - p_j||)$), not vector-based (i.e. $\varphi_{ij}^c(p_i - p_j)$), to allow for the rotational symmetry [16] of the N-VPs deformable flying object (see also the attached video clip); and 2) they rapidly increase when inter-VP/VP-obstacle collisions or inter-VP separation (e.g., with limited communication range) are impending to prevent that. For a design example of $\varphi_{ij}^c, \varphi_{ir}^o$, see Fig. 2.

The next Prop. 1 summarizes some key properties of the swarm behavior of the N VPs (5), with $\varphi_{ij}^c, \varphi_{ir}^o$ and bounded u_i^t. For that, define the Lyapunov function

$$V(t) := \frac{1}{2}\sum_{i=1}^{N}\sum_{j \in \mathcal{N}_i} \varphi_{ij}^c(||p_i - p_j||) + \sum_{i=1}^{N}\sum_{r \in \mathcal{O}_i} \varphi_{ir}^o(||p_i - p_r^o||)$$

and also assume that φ_{ij}^c and φ_{ir}^o are constructed s.t.: 1) there exists a large enough $\bar{M} > 0$ s.t. $V(t) \leq \bar{M}$ implies inter-VP connectivity preservation and no inter-VP/VP-obstacle collisions (e.g., rigid graph [13]); and 2) $\partial \varphi_{ij}^c / \partial p_i$ and $\partial \varphi_{ir}^o / \partial p_i$ are bounded, if φ_{ij}^c and φ_{ir}^o are bounded.

Proposition 1 *Suppose u_i^t is bounded with $||u_i^t|| \leq \bar{u}$ $\forall t \geq 0$, $\forall i \in \mathcal{N}_t \subset \{1, 2, .., N\}$ and $V(0) < \bar{M}$. Suppose further that, if $V(t) \geq \bar{M}$, there exists at least one VP, let's say the s^{th} VP, $s \in \{1, 2, ..., N\}$, s.t.*

$$\left\| \sum_{j \in \mathcal{N}_s} \frac{\partial \varphi_{sj}^c}{\partial p_s} + \sum_{r \in \mathcal{O}_s} \frac{\partial \varphi_{sr}^o}{\partial p_s} \right\| \geq \frac{\sqrt{N_t} + \delta_{st}}{2} \bar{u} \tag{8}$$

where N_t is the cardinality of $\mathcal{N}_t$; and $\delta_{st} = 1$ if $s \in \mathcal{N}_t$, and $\delta_{st} = 0$ otherwise. Then, all the N VPs are stable with bounded $\dot{p}_i$; inter-VP/VP-obstacle collisions are avoided; and inter-VP connectivity is preserved. Moreover, if $\varphi_{ir}^o = 0$ $\forall i \in \{1, 2, ...N\}$, $\sum_{i=1}^{N} \dot{p}_i = N_t \cdot u_i^t$ $\forall t \geq 0$.

[2]How to quantify this "denseness" of G to ensure no inter-VP collision is an interesting topic, and will be studied in future studies.

Proof: Differentiating the above $V(t)$, we have

$$\frac{dV}{dt} = \frac{1}{2}\sum_{i=1}^{N}\sum_{j\in\mathcal{N}_i}\left(\frac{\partial\varphi_{ij}^c}{\partial p_i}\dot{p}_i + \frac{\partial\varphi_{ij}^c}{\partial p_j}\dot{p}_j\right) + \sum_{i=1}^{N}\sum_{r\in\mathcal{O}_i}\frac{\partial\varphi_{ir}^o}{\partial p_i}\dot{p}_i$$
$$= \sum_{i=1}^{N}\underbrace{\left(\sum_{j\in\mathcal{N}_i}\frac{\partial\varphi_{ij}^c}{\partial p_i} + \sum_{r\in\mathcal{O}_i}\frac{\partial\varphi_{ir}^o}{\partial p_i}\right)}_{=:W_i^T}\dot{p}_i = \sum_{i=1}^{N}W_i^T\dot{p}_i$$

where we use $\dot{p}_r^o = 0$ (i.e., static obstacles) and

$$\sum_{i=1}^{N}\sum_{j\in\mathcal{N}_i}\frac{\partial\varphi_{ij}^c}{\partial p_i}\dot{p}_i = \sum_{i=1}^{N}\sum_{j\in\mathcal{N}_i}\frac{\partial\varphi_{ij}^c}{\partial p_j}\dot{p}_j \tag{9}$$

which is because, with $\varphi_{ij}^c = \varphi_{ji}^c$, the left term and the right term of (9) represent the same entity (i.e., $(\partial\varphi_{ij}^c/\partial p_i)\dot{p}_i$ and $(\partial\varphi_{ji}^c/\partial p_j)\dot{p}_j$), summed up respectively along the head set $\mathcal{H}(G) := \{i \mid (j,i) \in \mathcal{E}(\mathcal{G})\}$ and the tail set $\mathcal{T}(G) := \{j \mid (j,i) \in \mathcal{E}(\mathcal{G})\}$, yet, for the undirected G, $\mathcal{H}(G) = \mathcal{T}(G)$.

Then, injecting (5) into dV/dt with the definition of W_i above, we can obtain

$$\frac{dV}{dt} = \sum_{i=1}^{N}W_i^T(-W_i + u_i^t) \le \sum_{i=1}^{N}(-||W_i||^2 + \delta_{it}\bar{u}||W_i||)$$

where $u_i^t = 0$ if $i \notin \mathcal{N}_t$, $\bar{u} \ge ||u_i^t||$, and $\delta_{it} = \{1, 0\}$ is defined above. Now, suppose that $V(t) \ge \bar{M}$. Then, from (8), $\exists\ s \in \{1, 2, ..., N\}$ s.t. $||W_s|| \ge \bar{u}(\sqrt{N_t} + \delta_{st})/2$. Thus, we can show that

$$\frac{dV}{dt} \le -\sum_{i\notin\mathcal{N}_t^s}||W_i||^2 - ||W_s||^2 + \delta_{st}\bar{u}||W_s|| + \frac{(N_t-\delta_{st})\bar{u}^2}{4}$$
$$\le -\left(||W_s|| - \frac{\delta_{st}\bar{u}}{2}\right)^2 + N_t\frac{\bar{u}^2}{4} \le 0 \tag{10}$$

where $\mathcal{N}_t^s := \mathcal{N} \cup \{s\}$ and we use the facts that $\delta_{st}^2 = \delta_{st}$ and $-||W_i||^2 + \bar{u}||W_i|| \le \bar{u}^2/4$. This shows that $V(t) \le \bar{M}$ $\forall t \ge 0$, proving inter-VP/VP-obstacle collision avoidance and inter-VP connectivity preservation; and boundedness of $\dot{p}_i$ from (5), with bounded u_i^c, u_i^o (from bounded $\varphi_{ij}^c, \varphi_{ir}^o$ — see the assumption before Prop. 1) and bounded u_i^t.

Lastly, observe that, using the same reasoning for (9),we have $\sum_{i=1}^{N}\sum_{j\in\mathcal{N}_i}\partial\varphi_{ij}^c/\partial p_i = \sum_{i=1}^{N}\sum_{j\in\mathcal{N}_i}\partial\varphi_{ji}^c/\partial p_j$. Thus, by summing (5) for the all VPs, we have

$$\sum_{i=1}^{N}\dot{p}_i = \frac{1}{2}\sum_{i=1}^{N}\sum_{j\in\mathcal{N}_i}\left[\frac{\partial\varphi_{ij}^c}{\partial p_i} + \frac{\partial\varphi_{ij}^c}{\partial p_j}\right]^T + \sum_{i=1}^{N}u_i^o + \sum_{i\in\mathcal{N}_t}u_i^t \tag{11}$$

where the first term of RHS is zero since $\partial\varphi_{ij}^c/\partial p_i = -\partial\varphi_{ij}^c/\partial p_j$; and the second term is also zero if $\varphi_{ir}^o = 0$. ■

The assumption (8) of Prop. 1 is mild, since it just rules out the practically improbable (zero-measure) situation, where, although $V(t)$ is very large, *none* of the VPs can detect that, with all of their (also likely very large) forces, $\partial\varphi_{ij}^c/\partial p_i$ and $\partial\varphi_{ir}^o/\partial p_i$, are somehow exactly aligned with each other to make their sum nonetheless to be small. Note that, even without this detectability-like assumption (8), from (10), the growth of $V(t)$ would still be bounded by $\bar{u}^2 N_t/4$. See [17], where a result similar to Prop. 1 was achieved by using a sliding mode control approach.

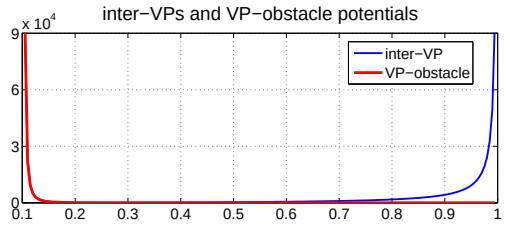

Fig. 2. Examples of φ_{ij}^c and φ_{ir}^o, to ensure VP-VP/VP-obstacle collision distance > 0.1 and VP-VP separation distance < 1 [11], [15].

Prop. 1 also says that: 1) all the N VPs will be stable (i.e., bounded $\dot{p}_i$), as long as u_i^t are bounded, regardless of whether u_i^t is used for some or all of the VPs; and 2) the more VPs implement u_i^t, the easier it would be to drive the N-VPs deformable flying object (e.g., centroid velocity $\sum_{i=1}^{N}\dot{p}_i$). In the next Sec. II-D, utilizing Prop. 1 and passive set-position modulation (PSPM [5]), we will design the teleoperation layer, which enables a remote human user to stably tele-control the velocity of the N VPs (5) via the master device (4) over the Internet with some useful haptic feedback.

Our usage of VPs is inspired by [8]. Yet, instead of the second-order dynamic VPs in [8], we choose the simpler first-order kinematic VPs (5), since 1) we can simplify/strengthen the VPs' swarm control design/analysis (e.g., stability of Prop. 1 valid with *any* bounded u_i^t for *any* VPs); and 2) we can avoid some performance-limiting aspects frequent with the dynamic VPs (e.g., operator's continuous exercise against the system/control damping [8], conservative passivity argument to enforce stability). See also [18], [19] for other "kinematic" abstractions.

D. PSPM-Based Teleoperation Layer

For the teleoperation layer, we utilize passive set-position modulation (PSPM) framework [5], whose passifying action will theoretically guarantee master-passivity/VPs-stability of the closed-loop teleoperation system over the Internet (with delay, loss, etc) with some useful haptic feedback, while whose flexibility will allow us to address kinematic/dynamic dissimilarity between the master device (4) (i.e., second-order Lagrangian dynamics with bounded workspace) and the VPs (5) (i.e., first-order kinematic system with unbounded workspace) and also to choose various forms of haptic feedback without jeopardizing the master-passivity/VPs-stability. PSPM also often exhibits better performance than other "time-invariant' teleoepration schemes (e.g. wave/PD) due to its less conservative "selective" passifying action. Our treatment on PSPM here is brief - see [5], [20] for more details.

First, to enable a remote human user to tele-control the VPs in $\mathcal{N}_t$, we define u_i^t in (5) s.t., for $t \in [t_k^i, t_{k+1}^i)$,

$$u_i^t(t) := \lambda q(k), \quad \forall i \in \mathcal{N}_t \tag{12}$$

where $q(k)$ is the master position $q(t) \in \Re^3$ received from the Internet at the i^{th} VP's reception time t_k^i, and $\lambda > 0$ is to match different scales between q and $\dot{p}_i$. The control (12) enables the user to tele-control the VP's velocity $\dot{p}_i$ via the master device position q, thereby, allows us to circumvent the master-slave kinematic dissimilarity [10] (i.e., mobile VPs with unbounded workspace; master device with bounded workspace). Note also that, if $q(t)$ is bounded, so will be $q(k)$. Thus, from Prop. 1, all the VPs (and UAVs) will be stable, if we can render $q(t)$ to be bounded, which will be achieved by PSPM below.

On the other hand, to allow the remote user to tele-sense some (or all) of the UAVs and obstacles, we design the haptic feedback signal $y(t) \in \Re^3$ to be sent to the master, s.t.

$$y(t) := \frac{1}{\lambda N_s} \sum_{i \in \mathcal{N}_s} (\dot{x}_i + u_i^o) \tag{13}$$

where $\mathcal{N}_s \subset \{1, 2, ..., N\}$ is the "sensing" subset among the N UAVs with $N_s > 0$ being its cardinality, $\dot{x}_i$ is the i^{th} UAV's velocity (1), and u_i^o is the i^{th} VP's obstacle avoidance control (7). This $y(t)$ is designed to allow the user: 1) to directly perceive the state of the *real* UAVs, thereby, completes the "information closed-loop" (i.e. master $\rightarrow$ VPs $\rightarrow$ UAVs $\rightarrow$ master) to overcome the unilaterality of the UAV control layer (e.g., prevent tele-driving VPs without knowing UAVs left behind due to, e.g., actuator failures) and also; 2) to sense the presence of obstacles via their collective effects on the VPs/UAVs in $\mathcal{N}_s$.

This $y(t)$ is then sent to the master over the Internet. Let us denote by $y(k)$ its reception by the master side over the Internet at the (master) reception time t_k. We incorporate this $y(k)$ into the teleoperation control τ in (4) s.t.

$$\tau(t) := -B\dot{q} - K_f q - K(q - \bar{y}(k)) \tag{14}$$

for $t \in [t_k, t_{k+1})$, where $B, K, K_f \succ 0$ are the diagonal gain matrices, and $\bar{y}(k)$ is the PSPM-modulation of $y(k)$ (to be defined below). This control (14) is designed s.t.: 1) if the UAVs fleet reaches the commanded velocity, the user will perceive this steady-state UAVs' velocity haptically (via f, unless $N_t = N$ and $K_f = 0$) and visually (by seeing q); and 2) if the UAVs fleet approaches to obstacles, the user will haptically perceive these obstacles by perceiving their collective feedback $\sum_{i=1}^N u_i^o$ in y. See item 2 of Th. 1. For simplicity, in this paper, we assume $\mathcal{N}_s = \{1, 2, ...N\}$ and $K_f = 0$, although other cases are also easily incorporatable.

At each t_k, $\bar{y}(k)$ in (14) is modulated via PSPM s.t.

$$\min_{\bar{y}(k)} \quad ||y(k) - \bar{y}(k)||$$
$$\text{subj. } E(k) = E(k-1) + D_{\min}(k-1) - \Delta\bar{P}(k) \geq 0$$

to enforce passivity, which would be violated if we directly utilize (switching) $y(k)$ in (14) without any remedy. Here, $E(k) \geq 0$ is the virtual energy reservoir; $\Delta\bar{P}(k) := ||q(t_k) - \bar{y}(k)||_K^2/2 - ||q(t_k) - \bar{y}(k-1)||_K^2/2$ with $||x||_A^2 := x^T A x$; and $D_{\min}(k) := \frac{1}{t_{k+1} - t_k} \sum_{i=1}^3 b_i (\bar{q}_i(k) - \underline{q}_i(k))^2$, with $b_i > 0$ being the i^{th} diagonal element of B, q_i the i^{th} element of q, and $\bar{q}_i(k)/\underline{q}_i(k)$ the max/min of $q_i(t)$ during $[t_k, t_{k+1})$, $i = 1, 2, 3$. Note that this PSPM is implemented only for the master side. Also, since the human operator usually keeps injecting energy into the master, $E(k)$ may keep increasing as well. To avoid excessive energy accumulation in $E(k)$, we ceil off $E(k)$, by discarding any energy over a certain threshold $\bar{E}$. See [5] for more details on PSPM. We now present the main result of this paper.

Theorem 1 *1) Consider the N VPs* (5) *and the master device* (4) *with the PSPM-modulated teleoperation control* (14)*. Then, the closed-loop master system is passive: $\exists$ $c_1 \in \Re$ s.t., $\int_0^T f^T \dot{q} dt \geq -c_1^2$, $\forall T \geq 0$. Moreover, if the human user is passive (i.e., $\exists$ $c_2 \in \Re$ s.t., $\int_0^T f^T \dot{q} dt \leq c_2^2$, $\forall T \geq 0$), all the VPs are stable, with $\dot{q}$, q, $q - \bar{y}(k)$, and $\dot{p}_i$ being all bounded.*

2) Suppose further that $\ddot{q}, \dot{q} \rightarrow 0$, $\mathcal{N}_s = \{1, 2, ..., N\}$, $E(k) > 0$ $\forall k \geq 0$, and $(x_i, \dot{x}_i) = (p_i, \dot{p}_i)$. Then, (a) if $\sum_{i=1}^N u_i^o = 0$ (e.g., no obstacles), human will have collective velocity haptic perception, s.t.

$$q(t) \rightarrow \frac{1}{\lambda N_t} \sum_{i=1}^N \dot{x}_i, \quad f(t) \rightarrow \frac{K}{\lambda} \frac{N - N_t}{N N_t} \sum_{i=1}^N \dot{x}_i$$

or, (b) if $\sum_{i=1}^N \dot{x}_i = 0$ (e.g., stopped by obstacles), human will have collective obstacle haptic perception, s.t.

$$f(t) \rightarrow -\frac{K}{\lambda} \frac{N + N_t}{N N_t} \sum_{i=1}^N u_i^o, \quad q(t) \rightarrow -\frac{1}{\lambda N_t} \sum_{i=1}^N u_i^o.$$

Proof: First, following the same procedure of [5, Th.1], we can show that: $\forall T \geq 0$,

$$\int_0^T f^T \dot{x} dt \geq V_m(T) - V_m(0) + E(\bar{N}) - E(0) \tag{15}$$

where $V_m(t) := ||\dot{q}||_M^2/2 + ||q(t_k) - \bar{y}(k)||_K^2/2$, and $\bar{N}$ is the k-index happening just before T. Using (15), we can then show: 1) master-side passivity (with $c_1^2 := V_m(0) + E(0)$); and 2) closed-loop VPs teleoperation stability, with LHS of (15) bounded by c_2^2 (from human passivity) and by using Prop. 1 (with bounded $u_i^t = \lambda q(k)$ from (12)).

For the item 2), with $\ddot{q}, \dot{q} \rightarrow 0$ and $E(k) > 0$ (i.e. $\bar{y}(k) = y(k)$), the closed-loop master dynamics becomes

$$K(q - y(k)) \rightarrow f(t) \tag{16}$$

with $q(t) \rightarrow q$. Moreover, from (11) with (12) and $\dot{p}_i = \dot{x}_i$, we have: $\sum_{i=1}^N \dot{x}_i \rightarrow \lambda N_t q$ [for 2)-(a)] or $\sum_{i=1}^N u_i^o \rightarrow -\lambda N_t q$ [for 2)-(b)]. From (13), we also have: $y(k) \rightarrow \sum_{i=1}^N \dot{x}_i/(\lambda N)$ [for 2)-(a)] or $y(k) \rightarrow \sum_{i=1}^N u_i^o/(\lambda N)$. Observing these and applying these to (16), we can then complete the proof. ■

We believe the master-passivity/VPs-stability of item 1) of Th. 1 is more suitable here than the usual master/slave-passivity, since 1) it does not require the human user to continuously overcome the damping dissipations in the VPs simulation and the UAVs dynamics (e.g., wind drag [8]); and 2) enforcing VPs' passivity is not so important here

(since not interacting with unknown environments: master device does so though) and even possibly detrimental (e.g., unnecessarily enforcing conservative passivity argument both for the master and the slave sides).

It is also worthwhile to mention that PSPM permits various forms of haptic feedback $y(t)$ other than (13) (e.g., $y := \dot{x}_l + 1/(\lambda N)\sum_{i=1}^{N} u_i^o$, where l represents a leader agent; or even nonlinear function $y := y(\dot{x}_i, u_i^o)$) while preserving the master-passivity/VPs-stability. Such a flexibility is usually not possible with other passivity-enforcing schemes (e.g. wave/PD). How to design a perceptually-optimized $y(t)$ is a very interesting problem. See [21] for a preliminary result in this direction. Note also that the disappearing haptic feedback of item 2a) of Th. 1 with $N_t = N$ can easily be recovered by using a non-zero K_f for (14).

III. SEMI-EXPERIMENTS

We used an Omega6® (Force Dimension) as a master derive with actuated linear 3-DOF and un-actuated rotational 3-DOF. Its local servo-loop runs at about 2.5 kHz on a Linux machine. A simulation environment was constructed to simulate UAVs dynamics and their control laws, by using Ogre3D engine (http://www.ogre3d.org/ for 3D rendering and computational geometry) and PhysX (http://www.nvidia.com/object/physx_new.html for simulating physical interaction). See Fig. 3. Our simulation runs at 60 Hz, creating asynchronous data update between the master device (i.e. 2.5kHz) and the slave UAVs (i.e. 60Hz), which produces some similarity with the Internet communication.

For the semi-experiment, we simulated $N = 8$ UAVs with all-to-all communication (complete graph G), and set the 28 inter-VP potentials φ_{ij}^c so as to realize a cubic shape with edge, edge diagonal, and cube diagonal measuring 3.3 [m], 4.67 [m], and 5.7 [m], as shown in Fig. 3. We also chose $\lambda = 10$ $[\mathrm{s}]^{-1}$, $K = 150$ [N/m], and $B = 2$ [Ns/m] for (12)-(14), and $E(0) = 2$ [J], $\bar{E} = 3$ [J] for the PSPM algorithm.

During the experiment, the user flew the UAVs in the simulated environment (with two walls installed at the left and right sides) twice from the side to side with almost a constant velocity, thus alternating 4 steady-state collective motion conditions, with 4 hard contacts with the walls (treated as obstacles). Behavior of the inter-VP distances is shown in Fig. 4, where we can see that: the UAVs start from the un-deformed cubic shape until about $t_1 = 1.9$ [s] when some of them get close to the first wall and their cubic shape deforms accordingly. Similar behaviors repeat after $t_2 = 5$ [s] when the UAVs move away from the wall and head towards the other wall (around $t_3 = 7.5$ [s]).

Fig. 5 contains the master position q (solid line) and the VPs' centroid velocity $\frac{1}{\lambda N}\sum_{i=1}^{N} \dot{p}_i$ (dashed line), showing a good teleoperation tracking performance when away from the walls. Fig. 6, on the other hand, depicts the master control force τ (top plot) and the average obstacle avoidance actions $\frac{1}{\lambda N}\sum_{i=1}^{N} u_i^o$ (bottom plot), showing a good haptic perception of the walls (i.e., obstacles). Finally, Fig. 7 (top) shows the UAV-VP tracking error $\|p_1 - x_1\|$ for the 1th UAV (similar plots for other UAVs omitted), and Fig. 7 (bottom) the

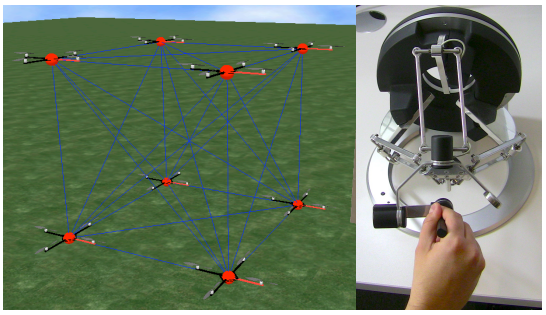

Fig. 3. UAVs in 3D simulation environment and master haptic device.

behavior of the PSPM virtual energy reservoir $E(k)$, which does not deplete (i.e., correct reproduction of the signal y) and drops to produce the obstacle haptic perception when the UAVs get close to the walls.

From these plots, we can then observe that:

1) stability of the closed-loop teleoperation system even with the asynchronous master-slave data update;
2) good teleoperation performance, with haptic perception of obstacles (Fig. 6) and human velocity command and UAVs' centroid velocity coordination (Fig. 5); and
3) good UAV-VP tracking performance as shown by the small $||p_1 - x_1||$ in Fig. 7.

See also the video clip attached to this paper for more realistic/interesting semi-experiment results.

IV. SUMMARY AND FUTURE RESEARCH

We propose a novel haptic teleoperation control framework for multiple UAVs, consisting of three layers: 1) UAV control layer to drive each UAV to follow its own VP; 2) VP control layer to render N VPs as a deformable flying object with inter-VP/VP-obstacle collision avoidance and inter-VP connectivity preservation; and 3) PSPM-based teleoperation layer to allow a human user to tele-control the bulk motion of N VPs with some useful haptic feedback over the Internet. Master-passivity/slave-stability and some asymptotic performance measures are proved. Semi-experiment results are also presented.

There are several possible future research directions: 1) reduction of the number of UAVs directly communicating with master while retaining performance level; 2) possibility of eliminating VPs; 3) full and more thorough experiments; and 4) perceptionally-optimized design of haptic feedback function y (13) - see [21].

ACKNOWLEDGMENTS

Research supported in part by the Max Planck Society and the WCU (World Class University) program through the National Research Foundation of Korea by the Ministry of Education, Science and Technology (R31-2008-000-10008-0). The authors also thank Johannes Lächele, Markus Ryll and Volker Grabe for their help in implementing and running the semi-experiments.

REFERENCES

[1] K. P. Valavanis, editor. *Advances in Unmanned Aerial Vehicles: State of the Art and the Road to Autonomy*. Springer, 2007. Intelligent Systems, Control and Automation: Science and Engineering, Vol. 33.

[2] R. Mahony and T. Hamel. Robust trajectory tracking for a scale model autonomous helicopter. *International Journal of Robust and Nonlinear Control*, 14:1035–1059, 2004.

[3] A. P. Aguiar and J. P. Hespanha. Trajectory-tracking and path-following of underactuated autonomous vehicles with parametric modeling uncertainty. *IEEE Transactions on Automatic Control*, 52(8):1362–1379, 2007.

[4] M-D. Hua, T. Hamel, P. Morin, and C. Samson. A control approach for thrust-propelled underactuated vehicles and its application to vtol drones. *IEEE Transactions on Automatic Control*, 54(8):1837–1853, 2009.

[5] D. J. Lee and K. Huang. Passive-set-position-modulation framework for interactive robotic systems. *IEEE Transactions on Robotics*, 26(2):354–369, 2010.

[6] P. Castillo, A. Dzul, and R. Lozano. Real-time stabilization and tracking of a four-rotor mini rotocraft. *IEEE Transactions on Control Systems Technology*, 12(4):510–516, 2004.

[7] T. M. Lam, M. Mulder, and M. M. van Paassen. Haptic feedback in uninhabited aerial vehicle teleoperation with time delay. *AIAA Journal of Guidance, Control & Dynamics*, 31(6):1728–1739, 2008.

[8] S. Stramigioli, R. Mahony, and P. Corke. A novel approach to haptic tele-operation of aerial robot vehicles. In *Proc. IEEE Int'l Conf. on Robotics & Automation*, pages 5302–5308, 2010.

[9] D. J. Lee and M. W. Spong. Bilateral teleoperation of multiple cooperative robots over delayed communication networks: theory. In *Proc. IEEE Int'l Conf. on Robotics & Automation*, pages 362–367, 2005.

[10] D. J. Lee and D. Xu. Feedback r-passivity of lagrangian systems for mobile robot teleoperation. In *Proc. IEEE Int'l Conf. on Robotics & Automation*, 2011. To appear.

[11] E. J. Rodriguez-Seda, J. J. Troy, C. A. Erignac, P. Murray, D. M. Stipanovic, and M. W. Spong. Bilateral teleoperation of multiple mobile agents: coordinated motion and collision avoidance. *IEEE Transactions on Control Systems Technology*, 18(4):984–992, 2010.

[12] D. J. Lee. Semi-autonomous teleoperation of multiple wheeled mobile robots over the internet. In *Proc. ASME Dynamic Systems & Control Conference*, pages 147–154, 2008.

[13] J. Aspnes, T. Eren, D. K. Goldenberg, A. S. Morse, W. Whiteley, B. D. O. Anderson, and P. N. Belhumeur. A theory of network localization. *IEEE Transactions on Mobile Computing*, 5(12):1663 – 1678, 2006.

[14] A. Franchi, P. Robuffo Giordano, C. Secchi, H. I. Son, and H. H. Bülthoff. A passivity-based decentralized approach for the bilateral teleoperation of a group of uavs with switching topology. In *Proc. IEEE Int'l Conf. on Robotics & Automation*, 2011. To appear.

[15] D. V. Dimarogonas and K. J. Kyriakopoulos. Connectedness preserving distributed swam aggregation for multiple kinematic robots. *IEEE Transactions on Robotics*, 24(5):1213–1223, 2008.

[16] P. Ogren, E. Fiorelli, and N. E. Leonard. Cooperative control of mobile sensor networks: Adaptive gradient climbing in a distributed environment. *IEEE Transactions on Automatic Control*, 49(8):1292–1302, 2004.

[17] Y. Cao and W. Ren. Distributed coordinated tracking via a variable structure approach - part ii: swarm tracking. In *Proc. American Control Conference*, pages 4750–4755, 2010.

[18] A. Sarlette, R. Sepulchre, and N. E. Leonard. Cooperative attitude synchronization in satellite swarms: a consensus approach. In *Proc. 17th IFAC Symp. on Automatic Control in Aerospace*, 2007.

[19] O. M. Palafox and M. W. Spong. Bilateral teleoperation of a formation of nonholonomic mobile robots under constant time delay. In *Proc. IEEE/RSJ Int'l Conf. on Intelligent Robots & Systems*, pages 2821–2826, 2009.

[20] Z. Zuo and D. J. Lee. Haptic tele-driving of a wheeled mobile robot over the internet: a pspm approach. In *Proc. IEEE Conference on Decision & Control*, pages 3614–3619, 2010.

[21] H. I. Son, J. Kim, L. Chuang, A. Franchi, P. Robuffo Giordano, D. J. Lee, and H. H. Bülthoff. An evaluation of haptic cues on the tele-operator's perceptual awareness of multiple uavs' environments. In *Proc. World Haptics Conference*, 2011. Submitted.

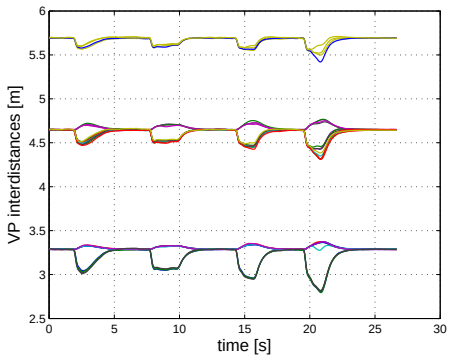

Fig. 4. Inter-VP distance: steady-state values corresponding to the undeformed N-VPs flying object shape.

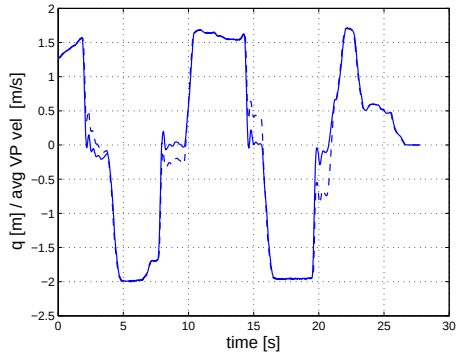

Fig. 5. Tele-coordination of $q(t)$ and $\frac{1}{\lambda N}\sum_{i=1}^{N}\dot{p}_i(t)$.

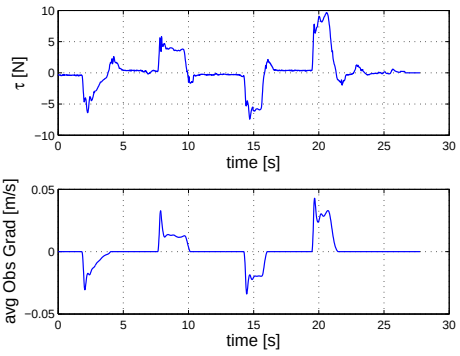

Fig. 6. Haptic perception of obstacles (i.e., $\frac{1}{\lambda N}\sum_{i=1}^{N}u_i^o(t)$) via $\tau(t)$.

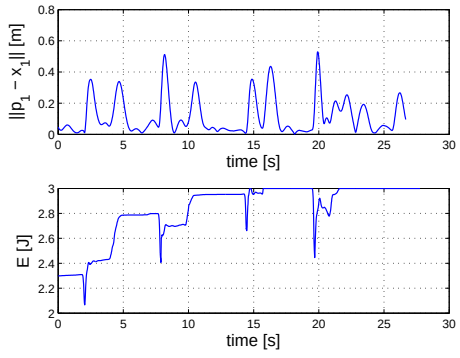

Fig. 7. UAV-VP tracking error $\|p_1(t)-x_1(t)\|$ and $E(k)$: note that small tracking error is maintained with $E(k)$ never depleting.